

Moving Mesh Application for Thermal-Hydraulic Analysis in Cable-In-Conduit-Conductors of KSTAR Superconducting Magnet

Qiuliang Wang, Keeman Kim

Samsung Advanced Institute of Technology, Moonji-dong, Yusong-gu, Taejon 305-380, Korea

Cheon Seog Yoon*

Department of Mechanical Engineering, Hannam University, Taejon 306-791, Korea

Jinliang He

Department of Electrical Engineering, Tsinghua University, Beijing 100080, China

In order to study the thermal-hydraulic behavior of the cable-in-conduit-conductor (CICC), a numerical model has been developed. In the model, the high heat transfer approximation between superconducting strands and supercritical helium is adopted. The strong coupling of heat transfer at the front of normal zone generates a contact discontinuity in temperature and density. In order to obtain the converged numerical solutions, a moving mesh method is used to capture the contact discontinuity in the short front region of the normal zone. The coupled equation is solved using the finite element method with the artificial viscosity term. Details of the numerical implementation are discussed and the validation of the code is performed for comparison of the results with those of GANDALF and QSAIT.

Key Words : Moving Mesh, Artificial Viscosity, Fusion Magnet, Quench Simulation, CICC

1. Introduction

A CICC is characterized by large stability margin, high breakdown voltage, good mechanical strength and smaller total mass of liquid helium required for cooling and low AC loss. For safe operation of the superconducting magnet, the protection from quenching is one of the important issues. Therefore, prediction of the quench characteristics, especially, the maximum supercritical helium pressure in the conduit, and hot-spot temperature of superconducting strands are essential for designing the magnet. The Korea Superconducting Tokamak Advanced Research (KSTAR) (Schultz, 1997) device is under con-

struction in Korea. The superconducting magnets for Toroidal Field (TF) and Poloidal Field (PF) will be fabricated using CICC's. The design value of the magnetic field strength at the center of the toroidal axis is 3.5 T (tesla). The TF and PF magnets should be able to operate in the complicated electromagnetic environment. Under the operating condition of KSTAR magnet system, the conductor temperature could rise over its current sharing temperature due to AC losses and the part of operating current pass through the stabilizer matrix and the Joule heat is generated. Depending on heat deposition and removal by convection and conduction, the superconductor is either recovered to the superconducting state or increased its temperature over the critical temperature to the normal state. The quench phenomena in the large-scale superconducting magnets fabricated using CICC have been studied in the past several years. For various applications, some numerical codes have been developed. The

* Corresponding Author,

E-mail : csyoon@mail.hannam.ac.kr

TEL : +82-42-629-8283; FAX : +82-42-629-8043

Department of Mechanical Engineering, Hannam University, Taejon 306-791, Korea, (Manuscript Received March 5, 2001; Revised January 2, 2002)

numerical solution of one-dimensional model was announced (Bottura, 1995). The basic numerical method includes the finite element method with artificial viscous damping term (Bottura, 1996), collocation method (Shaji, 1994), explicit finite element method (Bottura, 1991) and implicit finite difference (Koizumi, 1996) and finite volume algorithm with artificial viscosity (Wang, 1999). The numerical and analytical solutions show that the front of the normal zone in superconductor is characterized by a moving boundary and a contact discontinuity in temperature and density of supercritical helium (Shaji, 1996). It is difficult to obtain an accurate numerical solution, especially, in CICC's at high current and pulsed magnetic field zone. To simulate this phenomenon accurately, the adaptive refine meshes are required in the region, where the strong heat coupling occurs between the superconducting strands and supercritical helium.

The present method is the finite element method with moving mesh, and the artificial viscosity term is added. The model assumes a high heat transfer between the supercritical helium and superconducting strands. Therefore, the temperature of supercritical helium could be assumed to the temperature of superconducting strands (Luougo, 1998). Governing equations are the one-dimensional Navier-Stoke's equation for supercritical helium and the heat conduction equation for the conduit. The numerical implementation is introduced in this paper. The validation of the method is performed by proven numerical results. Finally, The quench analysis of the CICC for the KSTAR TF coil is carried out.

2. Physical and Mathematical Characteristics of Quench in CICC

The CICC contains superconducting strands, pure copper strands, supercritical helium and conduit, as in Fig. 1. While the length of the conductor for the Tokamak magnets is the dimension of 10^2-10^3 m, typically, the transverse scale of the CICC is the order of 10^{-2} m. Therefore, one-dimensional model is proper for the thermal hydraulic analysis. The thermal conduc-

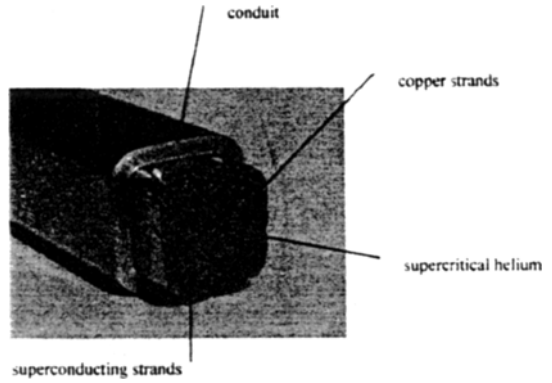


Fig. 1 KSTAR CICC configuration (superconducting strands, pure copper strands, supercritical helium, and conduit)

tion in supercritical helium is neglected since the effect of heat diffusion is much smaller than that of convection. Due to high heat transfer coefficient between the helium and superconducting strands and the large wetted perimeter of superconducting strands during quench of CICC, the temperature difference between the helium and superconducting strands is small and the temperatures of superconducting strands and helium are assumed to be the same. However, the temperature difference between the helium and the conduit should be taken into account, because of the small wetted perimeter of the conduit. The temperature distribution of the conduit is predicted by the energy equation. The coupled equations for supercritical helium, superconducting strands and conduit are expressed as;

$$M \frac{\partial \psi}{\partial t} + A \frac{\partial \psi}{\partial x} + B \psi = \frac{\partial}{\partial x} \left(K \frac{\partial \psi}{\partial x} \right) + G \quad (1)$$

Here, the matrix of the unknown, ψ , and coefficients matrix of the equations are defined as:

$$\psi = \begin{pmatrix} \rho \\ u \\ T \\ T_{jk} \end{pmatrix}, \quad M = \begin{pmatrix} 1 & 0 & 0 & 0 \\ 0 & \rho & 0 & 0 \\ 0 & 0 & \rho C_t & 0 \\ 0 & 0 & 0 & \gamma C_{jk} \end{pmatrix},$$

$$A = \begin{pmatrix} u & \rho & 0 & 0 \\ \frac{1}{\rho \alpha} & \rho u & \frac{\beta}{\alpha} & 0 \\ 0 & \left(\frac{A_{he}}{A_c} \right) \frac{\beta}{\alpha} T_{he} & \rho u C_v \left(\frac{A_{he}}{A_c} \right) & 0 \\ 0 & 0 & 0 & 0 \end{pmatrix},$$

$$K = \begin{pmatrix} 0 & 0 & 0 & 0 \\ 0 & 0 & 0 & 0 \\ 0 & 0 & k_{st} & 0 \\ 0 & 0 & 0 & k_{jk} \end{pmatrix},$$

$$B = \begin{pmatrix} 0 & 0 & 0 & 0 \\ 0 & f\rho \frac{|u|}{2d_h} & 0 & 0 \\ 0 & -f\rho \frac{|u|}{2d_h} \frac{u}{A_{he}} & \frac{p_{jk} h_{jk}}{A_c} & -\frac{p_{jk} h_{jk}}{A_c} \\ 0 & 0 & -\frac{p_{jk} h_{jk}}{A_{jk}} & \frac{p_{jk} h_{jk}}{A_{jk}} \end{pmatrix},$$

$$G = \begin{pmatrix} 0 \\ 0 \\ q_{dst} + q_{jst} \\ q_{djk} + q_{ijk} \end{pmatrix}$$

$$\rho C_t = \frac{A_{he}}{A_c} \rho C_v + \gamma C_{st}$$

In the equation, x and t are the coordinates for space and time, respectively. ρ , u and T are the density, velocity, and temperature of supercritical helium, respectively, and T_{jk} is the conduit temperature. α and β are the bulk compressibility and expansion coefficients of supercritical helium. C_v is the specific heat of supercritical helium at the constant volume, γC_{st} is the heat capacity of superconducting strands, and γC_{jk} is the heat capacity of conduit. k_{st} and k_{jk} are the thermal conductivity coefficients for superconducting strands and conduit, respectively. d_h is the thermal hydraulic diameter, and p_{jk} is the wetted perimeter of conduit, and A_c is the total cross-sectional area of superconducting strands and pure copper strands, A_{jk} is the cross sectional area of conduit, and A_{he} is the total cross sectional area of helium. h_{jk} is the heat transfer coefficient between the helium and conduit and f is the friction factor. q_{ijk} , q_{jst} , q_{djk} and q_{dst} are the Joule heat and disturbance power density in the conduit and superconducting strands, respectively. The equation includes the convection and diffusion terms. The coefficient matrix, K , is related to the thermal diffusion term of superconducting strands and conduit. It depends on the thermal conductivity of stabilizer matrix and conduit. The coefficient matrix, A , is connected to the convection terms of the supercritical helium. The source term includes the external heat

disturbance and Joule heating generation. The disturbance power, q_d , is with Gaussian distribution. The disturbance center is located at the L_0 and duration time, t_d .

$$q_d = \frac{q}{t_d} e^{-\pi \left(\frac{x-L_0}{L_d} \right)^2} \quad (2)$$

The total input energy of the disturbance is equivalent to that of a rectangular pulse with amplitude, q , and with disturbance length, L_d . The Joule heating power depends on the current sharing temperature, T_{sh} , and critical temperature, T_c , of superconducting strands. If the critical current is linearly varied with temperature, the Joule heating power is

$$q_{jst} = \begin{cases} 0 & (T < T_{sh}) \\ \frac{1+f_{cu}}{f_{cu}} \eta_{cu} J_{opt}^2 \frac{T-T_{sh}}{T_c-T_{sh}} & (T_{sh} \leq T \leq T_c) \\ \frac{1+f_{cu}}{f_{cu}} \eta_{cu} J_{opt}^2 & (T > T_c) \end{cases} \quad (3)$$

The Cu/SC ratio and full-current density of superconducting strands are f_{cu} and J_{opt} , respectively, and η_{cu} is the resistivity of stabilizer matrix.

3. Moving Mesh Finite Element Method for the Solution

The numerical algorithm for the coupled equation is presented in this part. The basic characteristics of Eq. (1) include the convection and diffusion terms. Apparently, the central difference or finite element method has instability for the high Reynolds number (Re). The flow velocity of supercritical helium is very low when the quench initiated, the typical value for the KSTAR magnet is lower than 0.1m/s (Anderson, 1984). If the normal zone is propagating, the maximum flow velocity of helium may be reached to the typical value of 10m/s or more. Therefore, while the normal zone is moving in the CICC, the convection term is the dominant heat transfer term. It is noted that this transition takes place continuously during the transient process. The front position of the normal zone, where the heat coupling is very strong, is moving. The moving boundary problem is a typical problem of free

boundary. The fine discretization of the region is necessary to solve transition accurately and to compute the propagation speed of the front, properly. The coupled equation of helium, superconducting strands and jacket is characterized by stiff mathematical nature. The thermo-physical properties for helium and material depend on the temperature and magnetic field, strongly. Therefore, the Eq. (1) is a highly nonlinear equation. The coupled Eq. (1) for the continuity, momentum and energy conservation equations of supercritical helium and conduit is rewritten as in Lagrangian form for the moving mesh problem (Blom, 1994)

$$\sum_{k=1}^{NPDE} C_{j,k}(x, t, \psi, \psi_x) \left(\frac{\partial \psi}{\partial t} - \frac{dx}{dt} \frac{\partial \psi}{\partial x} \right) = \frac{\partial}{\partial x} (R_j(x, t, \psi, \psi_x)) - Q_j(x, t, \psi, \psi_x) \quad (4)$$

for $j = 1, \dots, NPDE$, $x \in [x_L, x_R]$ and $t > 0$

where, NPDE is the number of variables, the solution, ψ , stands for $(\rho, u, T, T_{jk})^T$. R and Q are defined as flux and source terms, respectively, and dx/dt denotes the mesh velocity. Combined with Eqs. (1) and (4), the parameter, Q , is

$$Q = \left(\begin{array}{c} \rho \frac{\partial u}{\partial x} + u \frac{\partial \rho}{\partial x} \\ f \frac{|u|u}{2d_h} + \frac{1}{\rho^2 a} \frac{\partial \rho}{\partial x} + u \frac{\partial u}{\partial x} + \frac{\beta}{\rho a} \frac{\partial T}{\partial x} \\ \frac{A_{he}}{A_c} \rho C_p u \frac{\partial T}{\partial x} + \frac{A_{he}}{A_c} \beta \frac{\partial u}{\partial x} - \frac{A_{he}}{A_c} f \rho u \frac{|u|u^2}{2d_h} + \frac{p_{jk} h}{A_c} (T - T_{jk}) - Q_m - Q_d \\ - \frac{p_{jk} h}{A_c} (T - T_{jk}) - Q_{jk} \end{array} \right) \quad (5)$$

The finite element solution of the discretized equations is unstable. It is necessary to add the artificial viscosity to stabilize the oscillation of solution. The artificial viscosity with $\partial(k_v \partial \psi / \partial x) / \partial x$ is added to the Eq. (4). The coefficient term, C , and the flux term, R , are revised as, respectively

$$C = \begin{pmatrix} 1 & 0 & 0 & 0 \\ 0 & 1 & 0 & 0 \\ 0 & 0 & \rho C_t & 0 \\ 0 & 0 & 0 & \gamma C_{jk} \end{pmatrix}$$

and

$$R = \left(\begin{array}{c} \frac{1}{2} \alpha_\rho |u| \Delta x \frac{\partial \rho}{\partial x} \\ \frac{1}{2} \alpha_u (|u| + C_{he}) \Delta x \frac{\partial u}{\partial x} \\ k_{st} \frac{\partial T}{\partial x} \\ k_{jk} \frac{\partial T_{jk}}{\partial x} \end{array} \right) \quad (6)$$

Here, the coefficients of α_u and α_ρ are defined as the number from 0 to 1. The momentum equation adds the viscous term in the regime of the sound velocity, C_{he} , of supercritical helium. For mesh adaptation, the physical and computational spatial coordinates, x , and, ξ , respectively, are related by a differentiable monotone coordinate transformation,

$$x = x(\xi, t) \quad (7)$$

The moving mesh equation is constructed on the basis of so-called equal-distribution principle (Huang, 1994). When the large variations of solution occur, the monitor function, M , must be with some kind of smoothing the characteristics. This is handled by introducing an artificial diffusion term. The smoothed moving mesh equation is

$$\frac{\partial}{\partial \xi} \left(\frac{1}{M} \left(1 - \lambda^2 \frac{\partial^2}{\partial \xi^2} \right) (n \dot{u} + n) \right), \quad (8)$$

$$\lambda = \frac{N-1}{\sqrt{\gamma_m(\gamma_m+1)}} \text{ and } n = \frac{1}{\partial x / \partial \xi}$$

where τ is the time smoothing parameters, and γ_m is the spatial smoothing parameter with constant. Usually, these values are over than zero and more specific numbers are discussed in the part 5 of this paper. n is the so-called mesh concentration function, and the node number is N . The monitor function is chosen as follows;

$$M_i = \sqrt{\beta_m(t) + \sum_{j=1}^{NPDE} [(\bar{\psi}_{i+1} - \bar{\psi}_i) / (x_{i+1} - x_i)]^2},$$

$$\beta_m(t) = \beta_m(0) f_m(t) \text{ and } \bar{\psi}_i = \frac{\psi(x, t)}{\psi_m(x, t)} \quad (9)$$

Here $\beta_m(0)$ and $f_m(t)$ are the parameters used to control the mesh size and the numbers used here are 0.03 and 1, respectively. $\psi_m(x, t)$ denotes the maximum value for the each variables.

4. Boundary Condition and Initial Conditions, and Heat Transfer Coefficient

The initial and boundary conditions are needed to solve the discretized equations. In reality, CICC's in the superconducting magnet for the KSTAR system are generally connected with the constant pressure reservoirs at inlet and outlet. If P_{in} , P_{out} and T_{in} indicate the inlet and outlet pressures and inlet temperature of supercritical helium, respectively, the boundary conditions of constant pressure are given as follows;

$$\begin{aligned} P(\rho, T_{he}) &= P_{in} \\ \text{and } P(\rho, T_{he}) &= P_{out} \end{aligned} \quad (10)$$

The boundary conditions for the velocity of supercritical helium are determined on the basis of $\partial u / \partial x = 0$ at the inlet and outlet of CICC. The boundary condition of the temperature depends on the direction of velocity. During the supercritical helium flow into the CICC, i.e. the velocity of supercritical helium is positive and $T_{he} = T_{in}$ is set. Otherwise the adiabatic boundary conditions are imposed for the temperature in supercritical helium flow out of the CICC. The boundary condition of density depends on the boundary conditions of temperature and pressure. Under normal operation, the supercritical helium removes the steady-state heat flux in CICC, and the superconductor operates at the superconducting state. If a disturbance pulse is applied to the conductor, the transient thermal transfer will occur. Therefore, the initial condition is based on the steady state operating condition of superconducting magnets. The heat transfer coefficient between supercritical helium and conduit includes three components, i.e. the transient heat transfer coefficient, h_t , Kapitza conductance, and steady state heat transfer coefficient, h_s (Wang, 2000). Due to the large heating induced flow velocity, there exists a boundary of turbulence flow for supercritical helium in the CICC. The correlation of friction factors for the laminar and turbulence flow is based on the Reynolds number.

5. Numerical Experiments on Transient State Characteristics in CICC

The present analysis software, QSMFEM, uses a finite element method with moving mesh and adding artificial viscosity, and the verification of this code is performed by comparison with the Gandalf and QSAIT. The Gandalf of Cryosoft is a finite element code, which solves the fluid equations using an implicit stepping method (Bottura, 1996). The results of Gandalf have been demonstrated by the QUELL experiment (Marinucci, 1998). QSAIT, former developed by the authors, is based on the finite volume method with adaptive mesh and the fully implicit time integration of upwind scheme. It was tested with good accurate and fast execution speed (Wang, 2000). CICC's of TF superconducting magnets for KSTAR are selected for this study. The conductor has 486 Nb₃Sn superconducting and pure copper strands and 154 m in length for the cooling channel. The main parameters are listed in Table 1. The helium in the conduit has initial operating temperature of 5 K, pressure of 5 atm and zero mass flow rate. After the disturbance is imposed at the center of the conductor, the operating current is kept 1 s and then decayed with a time constant of 6.25 s. The disturbance length and duration time are 2 m and 10 ms, respectively.

Generally, for simulation of the thermal hydraulic characteristics in the CICC, the numerical approximations cause over-propagation of normal zone front position, therefore result in a non-linear process, which generates the numerical solution divergence from the physical one. The final results of the solution lead to a high velocity of the normal zone propagation and pressure region in the CICC. A converged solution can be obtained by (1) comparison of the numerical diffusion with the physical diffusion and (2) comparing the numerical results of repeating calculation for smaller step-sizes in space and time. In the simulation, the convergence of solution is studied for the space interval by the second method. In the code, QSMFEM, the time-step is adaptive. The first, the code predicts the

Table 1 Parameters of cable-in-conduit-conductors for KSTAR

| Conductor | Nb ₃ Sn | Conduit | Incoloy 908 |
|--------------------------------|--------------------|---------------------------------|--------------|
| Cu/non-copper | 1.5 | Conduit area (mm ²) | 244.6 |
| Strand diameter (mm) | 0.78 | Thickness of Cr (μm) | 1-2 |
| Strands number | 486 | Pure copper strands | 162 |
| Copper area (mm ²) | 170.3 | Non-Cu area (mm ²) | 62.9 |
| Helium area (mm ²) | 126.9 | Cable pattern | 3×3×3×3×6 |
| RRR | 100.0 | Longitudinal strain | -0.3% |
| Delay time (s) | 1.0 | Decay time (s) | 6.25 or 3.56 |
| Conduit wetted length (m) | 0.067 | Outlet pressure (atm) | 5. |
| Hydraulic diameter (mm) | 0.42 | Strands wetted length (m) | 1.19 |
| Maximum field (T) | 7.37 | Initial Mass flow rate (g/s) | 0 |
| Flow length (m) | 154 | Operating current (kA) | 35.16 |
| Disturbance length (m) | 2.0 | Disturbance duration (ms) | 10 |
| Pressure (atm) | 5 | Inlet temperature (K) | 5 |

solution using a backward differential formula (BDF) that represents the past history of each variable with a polynomial in time. The BDF polynomial has order of 1-5, and is automatically adjusted depending upon the characteristics of solution. It means that up to six past points enter into the prediction. After prediction of the solution, the Newton-iteration by a numerically evaluated Jacobian is used to converge the iteration. Therefore, the time step-size does not influence the convergence of the solution. However, the space interval is controlled by selection of various values, β_m . The minimum interval, Δx_{min} , in the front of normal zone influences the nature of the solution, significantly. Figs 2 and 3 show the convergence process of the solution for helium pressure and normal zone length with respect to time for various minimum intervals Δx_{min} . The profiles for helium pressure and normal zone length with respect to the time are kept constant under the minimum space interval in the normal zone front about 3.5 mm. The quench simulation of 2.5 s is studied by the several codes such as Gandalf, QSAIT and QSMFEM. In Gandalf, the total of 3000 elements with 2500 elements located at the center region of 20 m length is employed. In QSAIT, the size of the minimum mesh, $\Delta x_{min}=3.5$ mm, is assumed. The operating time step-size of integration is

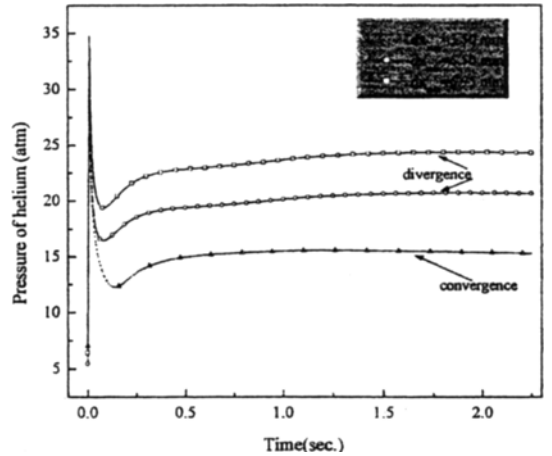


Fig. 2 Profiles of helium pressure with respect to time in various the space intervals

adaptive with maximum time interval of 0.45 ms. The code of QSMFEM takes the moving mesh with the node number of 401, the space smoothing parameter, $\gamma_m=2$, and the time smoothing parameter, $\tau=0.1$ ms. The $f_m(t)$ changes with the time based on the iteration number in each time step so as to keep $\Delta x_{min}=3.5$ mm. Though it is not clear to check the convergence tests for several combinations of space and time interval on Figs. 2 and 3, the space interval is controlled by various values of β_m , which influences on the solution convergence. Strict convergence test for details of

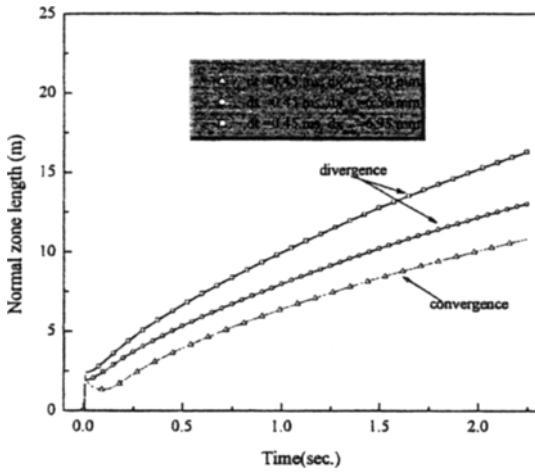


Fig. 3 Profiles of normal zone length with respect to time in various space intervals

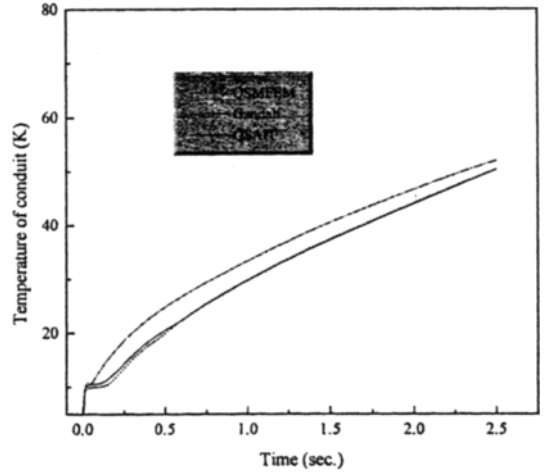


Fig. 5 Comparison for the profiles of conduit temperature with respect to time

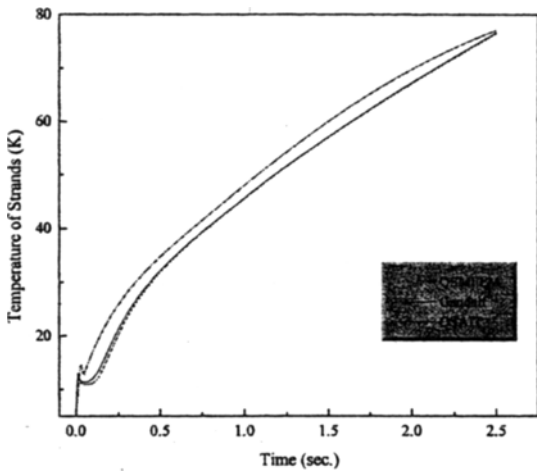


Fig. 4 Comparison for the hot spot temperature of superconducting strands with respect to time

β_m were shown on the author's other paper (Wang, 2002). Figures 4 and 5 show the hotspot temperatures of superconducting strands and conduit with respect to the time function, respectively. The difference of simulation results is small. In particular, the difference between QSMFEM and QSAIT is much smaller than that between QSMFEM and Gandalf. The difference between the QSMFEM and Gandalf is at initial time. After then, the difference tends to be reduced. Because the temperatures of superconducting strands and supercritical helium are not the same and treats separately in Gandalf, the

initial disturbance is directly deposited to the superconducting strands. On the other hand, the QSMFEM assumes that the temperatures of superconducting strands and supercritical helium are the same. Therefore, the initial disturbance is deposited to both the superconducting strands and supercritical helium. The heat capacity of single superconducting strands is smaller than that of the total heat capacity of superconducting strands and supercritical helium. With the disturbance absorbed by supercritical helium, the heating induced flow can significantly increase the heat transfer between the superconducting strands and helium. The temperature difference between superconducting strands and supercritical helium is dribbled away. The approximate model of high thermal transfer is much more complying with the practical process during quench in CICC.

Figures 6 and 7 show the profiles of the helium pressure and normal zone length with respect to time, respectively. From the results of simulation, the differences are varied small with the quench development in the CICC. It is noticed that the calculated pressure and normal zone length of Gandalf are slightly over than those of the QSAIT and QSMFEM. While QSAIT and QSMFEM use adaptive meshes and moving meshes to capture the normal zone front accurately, Gandalf uses fixed meshes at the normal zone front where steep

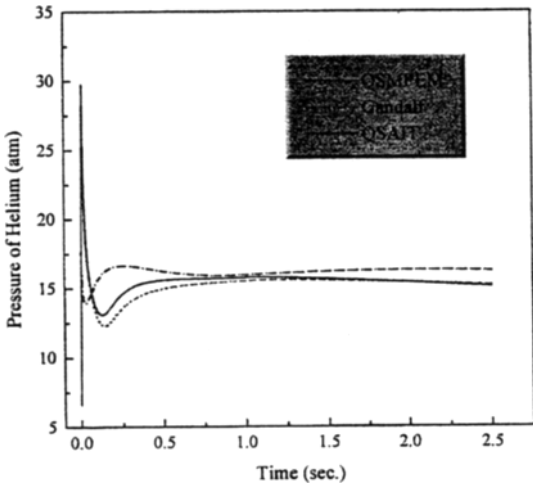


Fig. 6 Profiles of helium pressure with respect to time for the simulation by using Gandalf, QSAIT and QSMFEM

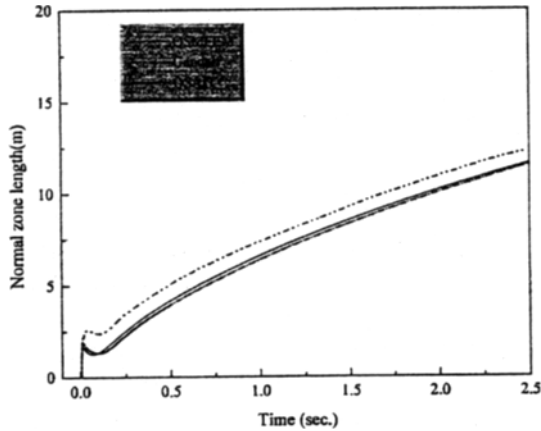


Fig. 7 Profiles of the extension of normal zone length for the simulation by using Gandalf, QSAIT and QSMFEM

gradient comes out. This is the reason why the results of Gandalf slightly overpredict. Also, it shows that the maximum pressure and normal zone length are sensitive to the mesh size at the front of normal zone.

For a long time simulation, the period of 6.5s transient process of quench in the CICC is studied by using QSMFEM. Figures 8, 9, 10 and 11 illustrate the space profiles for temperature of superconducting strands, pressure, density and thermal explosion velocity of supercritical helium

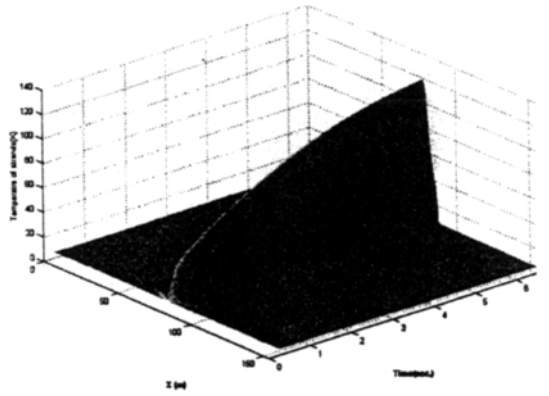


Fig. 8 Temperature profile of superconducting strands variation with the space and time for the KSTAR TF superconducting CICC during quench. The initial helium mass flow rate is zero

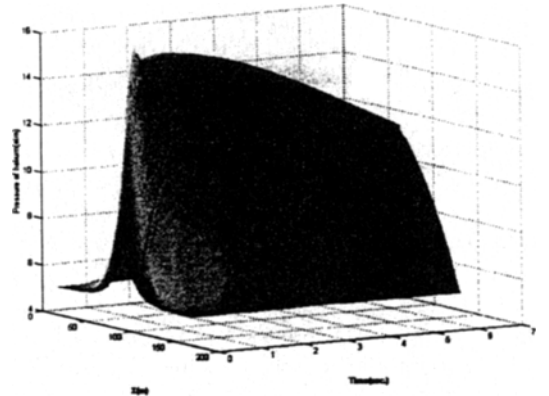


Fig. 9 Pressure profile of helium variation with the space and time for the KSTAR TF superconducting CICC during quench. The initial helium mass flow rate is zero

for disturbance length of 2m and disturbance duration of 10 ms by the QSMFEM, respectively. Figure 12 represents the mesh trace and the actual space mesh redistribution with the time. The redistribution of mesh is vital to achieve both the calculation efficiency and the accurate solution.

The decaying time constant of protection circuit is one of the important parameters. It has an influence on the hot spot temperature of CICC and the extension of the normal zone length. Figure 13 illustrates the profiles of the hot-spot temperature rise with respect to time in various

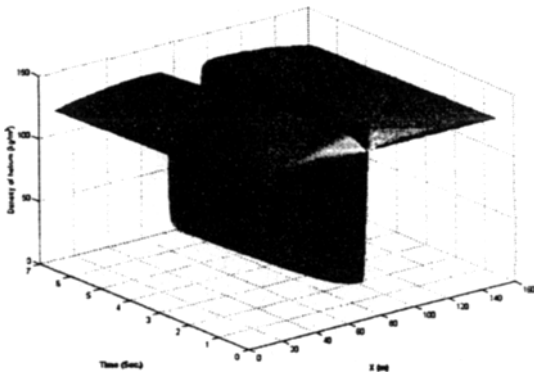


Fig. 10 Density profile of helium variation with the space and time for the KSTAR TF superconducting CICC during quench. The initial helium mass flow rate is zero

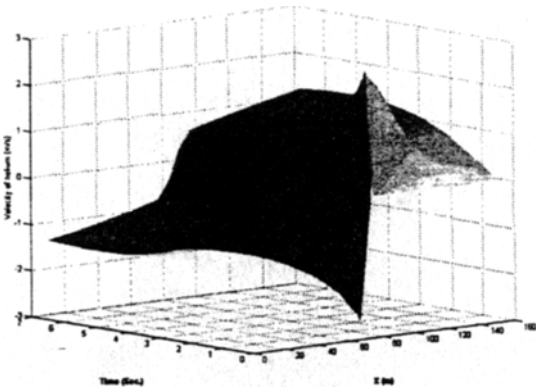


Fig. 11 Thermal explosion velocity profile of helium variation with the space and time for the KSTAR TF superconducting CICC during quench. The initial helium mass flow rate is zero

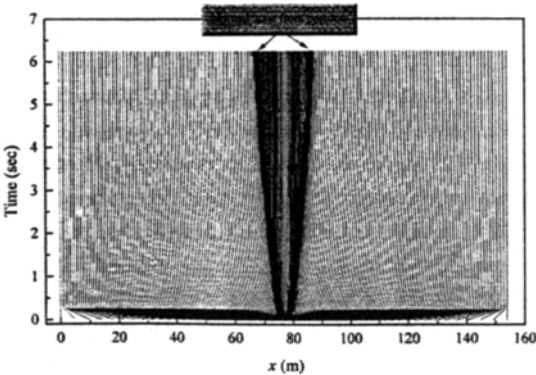


Fig. 12 Mesh trajectories, which start with initial non-uniform mesh, generated by moving mesh Eq. (8) for the quench simulation.

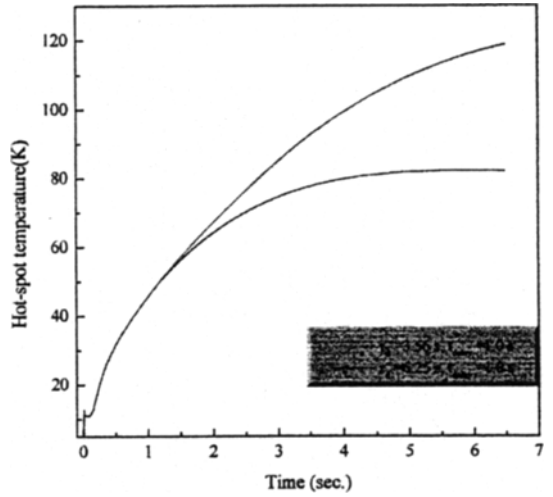


Fig. 13 Hot-spot temperature of the CICC with respect to time in various decaying time constant of protection circuit

decaying time constant. When the decaying time constant decreases from 6.25s to 3.56s, the hot spot temperature of the CICC is decreased from 119K to 80K.

6. Conclusions

A numerical method has been developed based on the finite element method with moving mesh. The model uses the high heat transfer approximation between the superconducting strands and supercritical helium. The code QSMFEM has following characteristics;

(1) The model can be used to analyze the quench characteristics of cable-in-conduit conductor. Thus, the code can be used to design large-scale superconducting magnets which are fabricated by CICC, such as Tokamak, superconducting magnet energy storage system etc.

(2) Using finite element method with moving mesh and artificial viscosity, the numerical instability can be pressed, and the method can capture the steep gradient of the solution. The fine mesh is located at the front region of normal zone. The simulation results of QSMFEM have shown the good agreement with those of the general numerical models.

(3) The time step is adaptive depending upon the nature of the solution so as to obtain the converged solution. The mesh size can be controlled by selecting the suitable function of $f_m(t)$. In addition, the method can be easily extended to three-dimensional problem and multi-cooling channel of superconducting magnet system.

(4) The significant physical solution is obtained by repeated calculation with the fine mesh at the normal zone front. The typical value is about 3.5–6 mm.

(5) The QSMFEM has a graphic interface. It is easy to observe the solution in the calculation by dynamic plot in each time step.

Acknowledgements

The work is supported by KSTAR project from Korean Ministry of Science and Technology. Authors thank Prof. Paul Zegeling who is working in the Department of Mathematics, Utrecht University in Netherlands for his advice about the numerical implementation for the moving mesh.

References

Anderson, D. A., Tannehill, J. C. and Pletcher, R. H., 1984, *Computational Fluid Mechanics and Heat Transfer*, Hemisphere Publishing Corporation.

Blom, J. G. and Zegeling, P. A., 1994, "Algorithm 731: A Moving Grid Interface for Systems of One Dimensional Time Dependent Partial Differential Equations," *ACM Transactions on Mathematical Software*, Vol. 20, pp. 194–214.

Bottura, L., EUR-FU XII/185/93.

Bottura, L., 1995, "Numerical Aspects in the Simulation of Thermo-Hydraulic Transients in CICC's," *Journal of Fusion Energy*, Vol. 14, pp. 13–24.

Bottura, L., 1996, "A Numerical Model for the Simulation of Quench in the ITER Magnets," *Journal of Computational Physics*, Vol. 125, pp. 26–41.

Bottura, L. and Zienkiewicz, O. C., 1991,

"Quench Analysis of Large Superconducting Magnets," *Cryogenics*, Vol. 32, pp.719–728.

Huang, W., Ren, Y. and Russell, R. D., 1994, "Moving Mesh Partial Differential Equations (MMPDEs) Based on the Equidistribution Principle," *SIAM Journal of Numerical Analysis*, Vol. 31, pp. 709–730.

Koizumi, N., Takahashi, Y. and Tsuji, H., 1996, "Numerical Model Using an Implicit Finite Difference Algorithm for the Stability Simulation of a Cable-In-Conduit Conductor," *Cryogenics*, Vol. 36, pp. 649–659.

Luogo, C. A., Loyd, R. J., Chen, F. K. and Peck, S. D., 1998, "Thermal Hydraulic Simulation of Helium Expulsion from a Cable-In-Conduit Conductor," *IEEE Transactions on Magnetics*, Vol. 25, pp. 1589–1595.

Marinucci, C., Bottura, L., Vecsey, G. and Zanino, R., 1998, "The QUELL Experiment as a Validation Tool for the Numerical Code Gandalf," *Cryogenics*, Vol. 38, pp. 467–477.

Schultz, J. H., 1997, "KSTAR Superconducting Magnets system," *KSTAR Design Point Definition Workshop*, Princeton Plasma Physics Laboratory, USA, pp. 205–243.

Shaji, A. and Freidberg, J. P., 1994, "Quench in Superconducting Magnets: I. Model and Numerical Implementation," *Journal of Applied Physics*, Vol. 76, pp. 3149–3158.

Shaji, A. and Freidberg, J. P., 1996, "Theory of Hybrid Contact Discontinuities," *Physical Review Letter*, Vol. 76, pp. 2710–2713.

Wang, Q., Oh, S., Ryu, K., Yoon, C. and Kim, K., 1999, "Numerical Analysis on Stability Margin and Quench Behavior in Cable-In-Conduit NbTi Conductor," *IEEE Transactions on Applied Superconductivity*, Vol. 9, pp.620–624.

Wang, Q., Yoon, C. S. and Kim, K., 2000, "Numerical Model for the Thermal-Hydraulic Analysis in the Cable-In-Conduit Conductor," *KSME International Journal*, Vol. 14, No. 9, pp. 985–996.

Wang, Q., He, J., Yoon, C. S., Chung, W. and Kim, K., 2002, "Simulation on Helium Expansion and Quench in CICC for KSTAR with Moving Mesh Methods," will be shown on *IEEE Transactions on Applied Superconductivity*, March.